Chinese Chemical Letters 31 (2020) 2071–2076

Contents lists available at ScienceDirect

Chinese Chemical Letters

journal homepage: www.elsevier.com/locate/cclet

Communication

Metal-organic frameworks-derived hierarchical ZnO structures as efficient sensing materials for formaldehyde detection

Nan Zhang, Luming Yan, Yang Lu, Yizhuo Fan, Sijia Guo, Samira Adimi, Dali Liu, Shengping Ruan*

State Key Laboratory on Integrated Optoelectronics and College of Electronic Science & Engineering, Jilin University, Changchun 130012, China

ARTICLE INFO

Article history:
Received 20 November 2019
Received in revised form 3 December 2019
Accepted 5 December 2019
Available online 5 December 2019

Keywords:
Metal-organic framework
ZIF-8
Formaldehyde sensing
Pore-rich structure
ZnO nanocubes

ABSTRACT

Semiconducting metal oxides have been considered as effective approach for designing high-performance chemical sensing materials. In this paper, a kind of metal-organic frameworks ZIF-8 was used as sacrificed template to prepare porous ZnO hollow nanocubes for the application in gas sensing. It is found that changing calcination temperature and solvent can greatly influence the morphology of the material, which finally affects the gas sensing performance. Acetylene-sensing properties of the sensors were investigated in detail. It can be clearly seen that the material used methanol as reaction solvent with the decomposition at 350 °C for 2 h (ZnO-350-M) showed the optimal formaldehyde-sensing behaviors compared with other materials prepared in this experiment. The dynamic transients of the ZnO-350-M-based sensors demonstrated a high response value (about 10), fast response and recovery rate (4 s and 4 s, respectively) and good selectivity towards 100 ppm (part per million) formaldehyde as well as a low detectable limit (1 ppm). As exemplified for the sensing investigation towards formaldehyde, the porous ZnO hollow nanocubes showed a significantly improved chemical sensitivity due to the highly synergistic effects from the well exposed surfaces, defect states and the robust ZnO.

In recent years, owing to the fact that toxic gases can cause damage to environment and physical health, a great deal of interest has been devoted to detection of toxic gases using various inorganic semiconductor oxides such as WO_3, Co_3O_4 and SnO_2 [1–3]. Formaldehyde, as a kind of the volatile organic compounds (VOCs), is the main indoor pollutant which could cause sick building syndrome (SBS) [4–6]. Hence, highly sensitive gas sensing materials with fast response/recovery speed are desirable in detection of formaldehyde. Semiconducting ZnO has been considered as one of the most promising gas sensing materials [7]. Different morphologies of ZnO, including nanoplates, nanotubes, nanofibers and microspheres have been synthesized by various convenient routes, such as hydrothermal synthesis, solvothermal routes, and vapor-solid growth [8–12]. As such, hollow nanostructured materials are investigated in gas sensing applications due to their unique structural properties of low mass density, surface permeability and shortened diffusion paths, which could maximize the interactions between the surface and gas molecules [13,14]. Metal organic frameworks (MOFs) materials, as a novel class of crystalline hybrid materials, are composed by coordinated inorganic clusters and organic bridging linkers [15]. Due to the unique chemical and physical properties such as ordered structures [16], large specific surface area, extra-high porosity [17] and adjustable chemical functionality [18], this type of materials become more and more attractive in an incredible range of potential applications, including gas absorption/ separation [19], drug delivery [20] as well as optical sensing [21], *etc*. Zeolite imidazolate frameworks (ZIFs) are one of the most intriguing MOF materials owing to its simple synthesis methods and excellent chemical and thermal stability [22]. At present, it is rarely reported to explore the effects of different solvents on the gas sensing performance of MOFs-derived metal oxide semiconductor synthesized by different reaction solvent.

In this paper, ZIF-8 prepared was served as sacrificial templates and metal precursors to constructing well-defined ZnO hollow nanocubes with high porosity. Due to the fact that morphology can influence the gas sensing performance [23], the influences of calcination temperature, heating rate and solvent have been taken into considerations in this experiment. After exploring these conditions, the porous ZnO hollow nanocubes with uniform and

* Corresponding author.
E-mail address: ruansp@jlu.edu.cn (S. Ruan).

https://doi.org/10.1016/j.cclet.2019.12.014
1001-8417/

ideal morphology were successfully prepared. The samples were highly sensitive towards formaldehyde with fast response/recovery time of less than 5 s.

ZIF-8 was prepared according to the previous reports [24,25] but with some modifications. In a typical synthesis, $Zn(NO_3)_2{\cdot}6H_2O$ (1.485 g) and 2-methylimidazole (1.642 g) were dissolved in 20 mL methanol, respectively, to form two clear solutions. Then, the above methanolic solution of $Zn(NO_3)_2{\cdot}6H_2O$ was slowly injected into the methanolic solution of 2-methylimidazole with continuous stirring for 5 min at room temperature, and then mixture was aged for 24 h at room temperature. The resulting white precipitates were collected by centrifugation, washed with alcohol for 3 times. After drying the samples at 60 °C for 12 h, the ZIF-8 was prepared. To explore the ideal condition of experiment, the solvent was replaced by DMF and ethanol, respectively.

The precursors of ZIF-8 were loaded in a ceramic crucible and heated to 300 °C with heating rate of 1 °C/min. After heating at 300 °C for 2 h, the material was prepared successfully. To find the satisfactory heating condition, the different calcination temperature from 300 °C to 350 °C and 400 °C was carried out in this experiment.

The as-prepared material was mixed with deionized water at a weight ratio of 4:1 and ground in a mortal to form a paste. Then the paste was coated on an Al_2O_3 ceramic tube with a couple of parallel Au electrode sprinted to form a sensing film (the thickness was about 300 μm). A Ni-Cr heating wire was inserted into the ceramic tube as a heater to control the operating temperature [26]. For a typical gas sensing test, gas sensing properties were measured by a chemical gas sensor-8 (CGS-8) intelligent gas sensing analysis system (Beijing Elite Tech Co., Ltd., China) under room condition (25 °C, 36% RH). Before testing, the sensors were aged in the air at 160 °C for 24 h to achieve stabilization of device. The response value (S) was defined as $S = R_a/R_g$, where R_a and R_g presented the resistance of sensor in the air and in the target gas, respectively. Response time and recovery time were defined as the time needed for 90% of total resistance change on exposure to the target gas and air, respectively [27].

X-ray diffraction (XRD) measurements were conducted to provide crystallinity and phase structures information of the synthesized materials. Fig. 1a showed the XRD patterns of the ZIF-8 precursors using different solvent. The diffraction peaks of MOF precursors were in good agreement with the stimulated ZIF-8. Fig. 1b showed the XRD patterns of the calcined products with calcination temperature of 300 °C. It revealed that the ZIF-8 was not transformed to other substance but still remained unchanged while being calcined at 300 °C. The XRD patterns of the products calcined at 350 °C and 400 °C were shown in Figs. 1c and d, respectively. It was shown that ZIF-8 was converted into ZnO when it was calcined at 350 °C or above. The main ZnO diffraction peaks were in good consistency with ZnO (JCPDS card No. 36-1451) and no other diffraction peaks corresponding to residues or contaminants were observed [28].

Typical morphology of the ZIF-8 precursors using the different solvent and materials calcined at 300 °C with the heating rate at 1 °C was shown in Figs. S1d-f (Supporting information). It could be seen that the size of ZIF-8 is influenced by changing the reaction solvent. Compared with materials using DMF or ethanol as reaction solvent, the nanocubes have smaller average size which is 200−300 nm when using methanol as solvent. It was shown that the samples retain a similar morphology to that of the ZnO ZIF

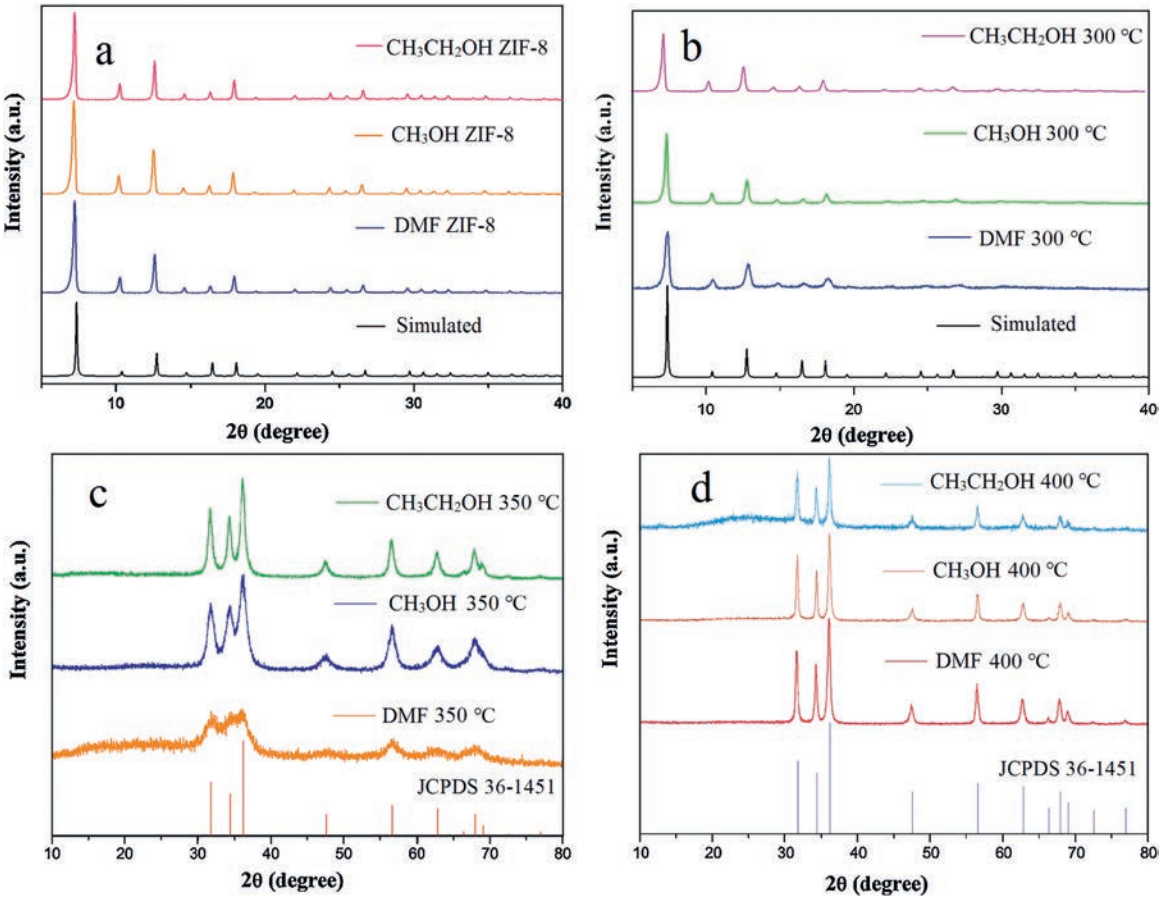

Fig. 1. (a) The XRD pattern of the ZIF-8 precursors using different solvent. The XRD pattern of the products calcined at (b) 300 °C , (c) 350 °C and (d) 400 °C.

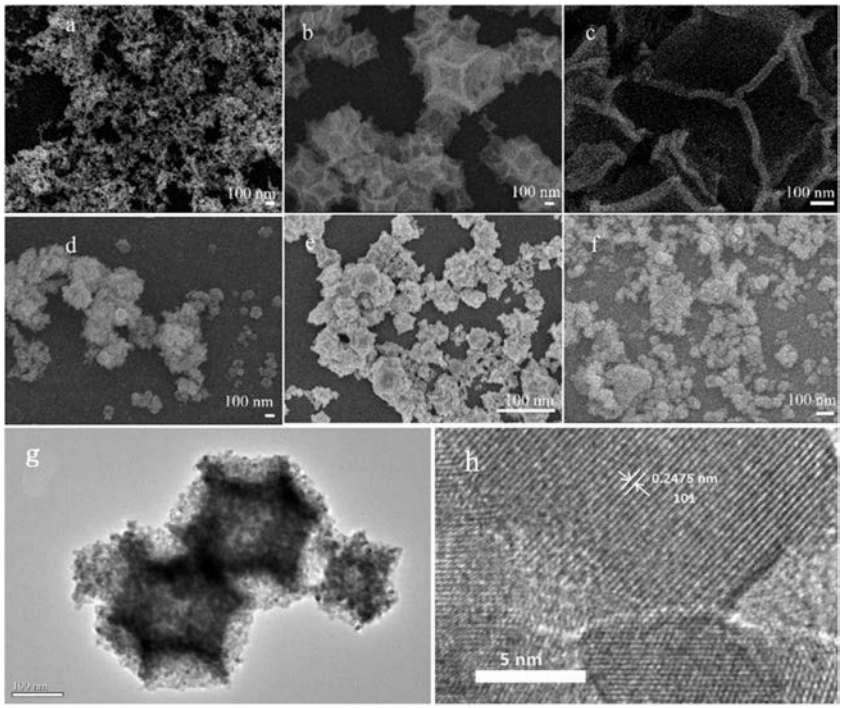

Fig. 2. SEM image of samples ZnO: (a) ZnO-350-D; (b) ZnO-350-M; (c) ZnO-350-E; (d) ZnO-400-D; (e) ZnO-400-M; (f) ZnO-400-E. (g) TEM image of ZnO-350-M; (h) HRTEM images of ZnO-350-M (101) planes.

templates after calcination. The TGA curves of ZIF-8 are shown in Fig. S2 (Supporting information). The TGA of ZIF-8 showed structural stability up to 200 °C. When the thermal treatment temperature exceeded 300 °C, the ZIF-8 precursor was transformed into ZnO. In addition, a total weight loss of about 55% in the temperature range of 200–400 °C indicated that ZnO was derived completely by thermal decomposition of the ZIF-8 structure. When the heating temperature was raised to 350 °C and 400 °C, respectively, the morphologies of polyhedron nanocubes changed considerably, as shown in Fig. 2. It could be seen from Figs. 2a-c that when DMF, methanol and ethanol served as reaction solution, the hollow nanocubes were uniform and depressed inward, and the surface of the particle became fairly rough. The nanocubes using methanol as solvent have smaller size compared with other material calcined at 350 °C. However, when the temperature was raised to 400 °C, the concave cubic morphology of all samples was almost disappeared, and most of them became quasi-spherical agglomerate. From those figures, it was clear to see that the material used methanol as reaction solvent with the calcination temperature at 350 °C and heating rate at 1 °C (ZnO-350-M) had the well-defined morphology compared with other materials. More detailed structural information of ZnO-350-M porous nanocubes was revealed by TEM characterization as shown in Figs. 2g and h. The projection profiles of most particles remained square with the edges concave, which was in consistent with the morphology in the SEM observation. It indicated that the cubic particles were extremely porous in the interior, and its diameter was about 100 nm. A close observation on an individual ZnO nanocube revealed that these concave nanocubes were composed of numerous crystallites with 5–10 nm in size, as shown in the Fig. 2g.

XPS analysis is employed to investigate the chemical composition and oxidation state in ZnO-350-M. As shown in Fig. 3a, the peaks of Zn and O are clearly observed in the full range spectra. In XPS Zn 2p spectra of the sample (Fig. 3b), the fitting Zn 2p peaks centered at ~1045.8 and ~1022.7 eV are in good correspondence with Zn $2p_{1/2}$ and Zn $2p_{3/2}$, revealing the Zn(II) oxidation state. The analysis of oxygen species is critical for chemical sensing materials. As shown in Fig. 3c, the O 1 s spectrum can be fitted into three peaks, including lattice oxygen species (O_{latt}), and adsorbed oxygen species (O_{ads}). Porous materials generally have a large surface area, which will be beneficial for improving gas sensing properties. As shown in Fig. 3d, we analyze the specific surface area (SSA) by the N_2 adsorption/desorption isotherm. The SSA of ZnO-350-M and ZnO-400-M were 56.4 and 27.3 m^2/g. A larger SSA provides more surface active sites to improve gas sensing performance. The pore size distribution (PSD) is shown in the inset of Fig. 3e, demonstrating that the peaks of PSD concentrate at about 16.9 and 22.1 nm. The gas sensing performance of material calcined at 350 °C was so unsatisfactory according to our experiment that it was unnecessary to explore its gas sensing properties. It was known to all that the operating temperature could greatly influence the gas sensing property of the sensor [29], so different operating temperatures were carried out to find out the optimal condition by testing the response of the sensor at 100 ppm formaldehyde. As shown in Fig. 4a, for samples after calcination at 350 °C, the responses of the sensors increased with increasing operating temperature at the beginning, and then decreased when the temperature continued increasing after getting a maximum value at 183 °C. As a result, the optimum operating temperature of the sensors based on ZnO-350-D, ZnO-350-M and ZnO-350-E were shown to be 230 °C, and the response value increased to 10 toward 100 ppm formaldehyde, which was nearly 2 times higher than that of ZnO-350-E sample. As shown in Fig. 4b, 206 °C was suggested to be the optimal operating temperature for ZnO-400-M and ZnO-400-E, while the optimal operating temperature based on ZnO-400-D was 160 °C. The sensing selectivity is also an important parameter for determining the gas sensing performance of sensors. The selectivity of sensors based on ZIF-derived materials using methanol as reaction solution was tested by exposing the sensor to 100 ppm potential interference gases such as methanol (CH_3OH), trimethylamine (C_3H_9N), acetylene (C_2H_2) and so on. From Fig. 4c,

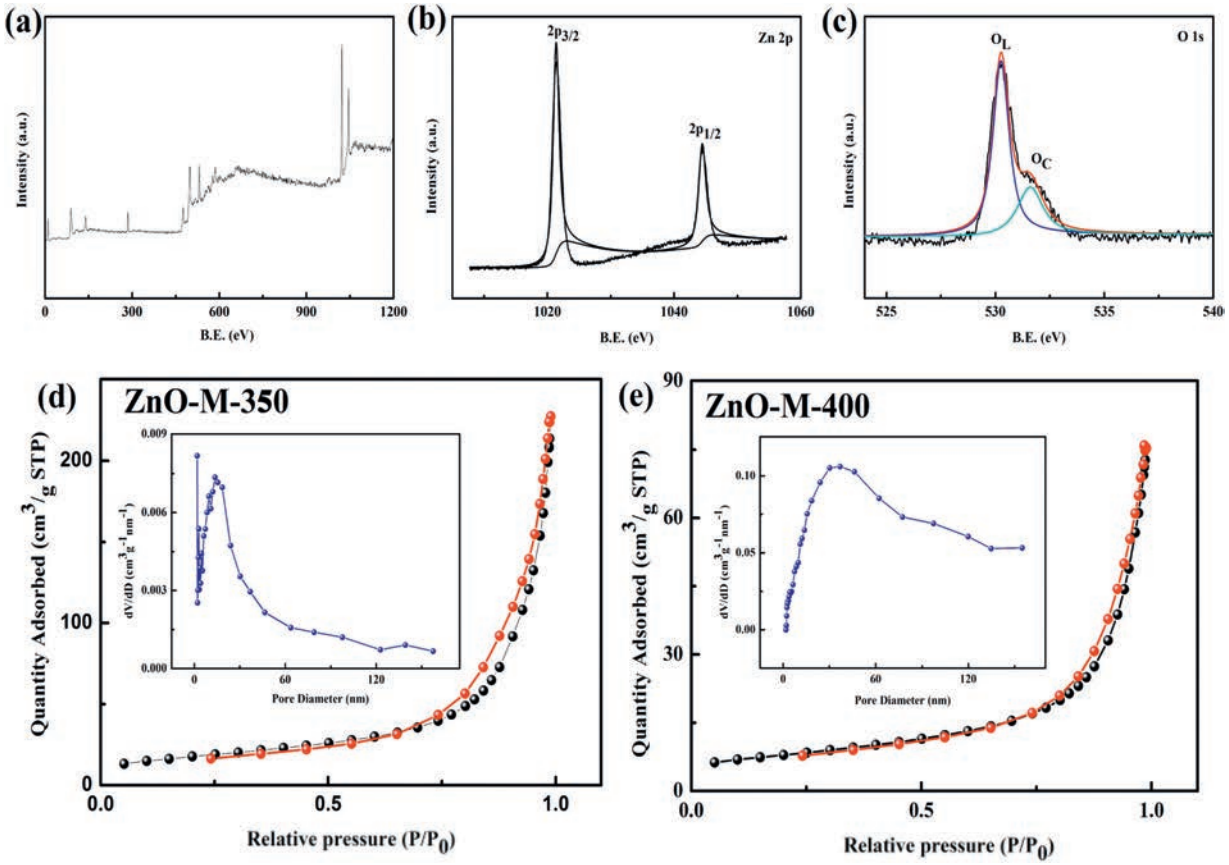

Fig. 3. (a) The complete XPS spectra of ZnO sample. XPS spectra in the vicinity of the (b) Zn 2p and (c) O 1s peaks. Nitrogen adsorption–desorption isotherms and pore size distributions of (d) ZnO-M-350 and (e) ZnO-M-400 sample.

it can be seen that the ZnO-350-M gas sensor exhibited excellent selectivity to formaldehyde compared with other gases at 183 °C.

To investigate the relationship between the concentration of target gas and the response of the sensor, the sensor was tested by being exposed to different concentrations of formaldehyde at the optimal operating temperature. As shown in Figs. 4d and e, the responses of these ZIF-derived materials obtained by calcination at 350 °C was higher than those of sensors based on the materials calcined at 400 °C. Through comparing these materials, ZnO-350-M displayed the highest response when exposed to each concentration of HCHO. The response increased rapidly with the increase of HCHO concentration from 10 ppm to 100 ppm and gradually slowed down from 200 ppm to 500 ppm. As shown in Fig. 4f, the response curve of the sensor as a function of the formaldehyde concentration (10–200 ppm) shows an almost linear trend. Hence, the approximation formulas are obtained by using linear regression analysis: $S = 0.07C + 2.24$ ($C \geq 10$), where S and C are the responses of sensor and the concentration of formaldehyde. According to the criterion about gas detection limit ($R_{air}/R_{gas} > 1.2$), the formaldehyde detection limit of the ZnO-350-M sensor is estimated to be 10 ppm.

It is generally known that response and recovery characteristics are critical for sensing properties of sensors. Figs. 4g and h showed the response and recovery times of different sensors which were used different reaction solution and calcined at different temperatures. The curves show that the sensors have good response/recovery characteristics and the response increases as the formaldehyde concentration increases from 10 ppm to 200 ppm. It could be seen from Fig. S3 (Supporting information) that when ZnO-350-M was exposed to 100 ppm formaldehyde, the response time was about 4 s, so was the recovery time. However, ZnO-350-E and -D exhibited longer response/recovery times of 5 s/7 s and 5 s/6 s, respectively. The remarkably shorter response-recovery time can be attributed to the hollow and porous structure, which can provide larger active surface area and accelerated diffusion path.

From Fig. 4i, the long-term stability of ZnO-350-M-based sensors was measured within 20 days, and it could be seen from the curve that the response exhibited a decrease of about 6.8%, which indicated a good long-term stability.

Table S1 (Supporting information) summarized the formaldehyde-sensing performances reported in references [30–34]. Until now, the formaldehyde sensors has been widely utilized, including ZnO/ZIF-8 nanorods, ZnO/ZIF-8 nanorods, SnO_2 nanosheets, In_2O_3 octahedron, and $Co_3O_4/CoFe_2O_4$ nanocubes. Our ZnO-ZnO-350 sensor has a low operating temperature (183 °C) and fast response and recovery speeds (4 s, 4 s). Thus, these good sensing performances make our sensor competitive when compared with other formaldehyde sensors.

ZnO is one of the most common n-type oxide semiconductor of gas sensing materials, its sensing mechanism can be explained by the change in electrical conductivity caused by the chemical interaction of gas molecules with the surface of the semiconductor metal oxides. When ZnO is exposed in air ambient, the oxygen will capture electrons from ZnO conduction band to generate oxygen species in the form of O_2^-(ads), O^- (ads) or O_2^{2-}(ads) on the surface of ZnO, which can lead to a decrease in conductivity [35].

In the formaldehyde ambient, formaldehyde molecules can react with the chemisorbed oxygen species and release the trapped

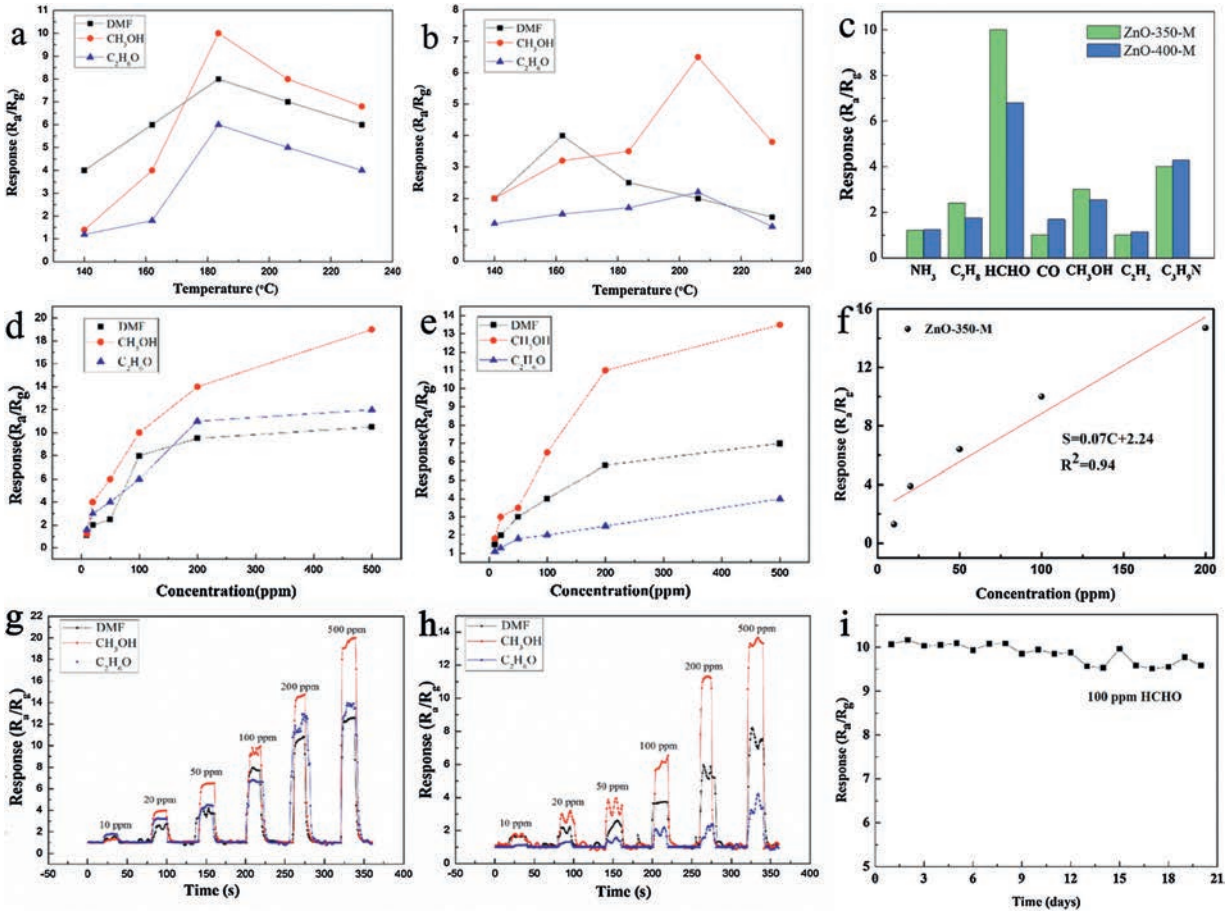

Fig. 4. Response of sensors based on ZnO using different solvent calcined (a) at 350 °C and (b) at 400 °C to 100 ppm formaldehyde at different temperatures. (c) Responses of sensors based on ZnO calcined at different temperature using different solvent at 183 °C to 100 ppm various gases. Response of sensors based on ZnO calcined at (d) 350 °C and (e) 400 °C at 183 °C to formaldehyde at different concentration. (f) Responses of the ZnO-350-M sensor as a function of low formaldehyde concentration (10–200 ppm). Response and recovery time of sensors based on ZnO calcined at (g) 350 °C and (h) 400 °C at 183 °C to formaldehyde at different concentration. (i) Long-term stability of the ZnO-350-M based sensor to 10 ppm formaldehyde at 183 °C.

electrons back to the conduction band of ZnO, which increases the carrier concentration and electron mobility, resulting in the decrease of sensor resistance. The reaction can be described as follows [36]:

$$HCHO + 2O^{-}(ads) \rightarrow CO_2 + H_2O + 2e^{-}$$

It is generally known that the morphology can influence the sensing properties of material, which may explain the reason ZnO-350-M based gas sensor had the better response and shorter response/recovery time. It can be found from Fig. 3 that changing the reaction solution can influence the size of the particles. It is confirmed that reducing the size of the material can improve the gas sensitive performance significantly through experiment [37]. Thus, the smaller size can be realized by using methanol as reaction solution, which results in higher response to formaldehyde. Moreover, the structure of ZnO-350-D is so compact compared to the other three porous samples according to the SEM analysis (Figs. 4a-c). Thus, the sensing speed of the ZnO-350-D (5 s/6 s) was long due to the detained gas diffusion.

Calcination temperature is also an important influence factor of sensing properties in this experiment. ZIF-8 is not altered to other substance when calcination temperature is below 350 °C, so there is still some organic matter in the polyhedron. The impurities prevent gases from reacting with sensitive layers, which results in extremely low response. When temperature is raised to 350 °C, the organic matter is burned up, then hollow and porous ZnO-350-M is formed. Hence, the gas molecules could freely pass into and out of the ZnO-350-M owing to their special structures. Consequently, on one hand, the hollow structure can reduce the agglomeration of particles [38], and formaldehyde can not only react on the surface of sensitive layer, but also react on the inner surface of material by entering into the hollow polyhedron, so that it may improve the gas utilization efficiency of material, leading to significant increase of the response. On the other hand, the hollow polyhedron is composed of a large number of nanoparticles, thus, it makes the surface more active and then enhance the ability of chemical adsorption and formation of ionized oxygen. As a result, more electrons are released, which improves the gas sensing performance to a better degree [39]. However, the morphology is destroyed when the temperature is raised to 400 °C. The particles are easily agglomerated to form larger size of secondary particles. So, it makes target gas difficult to spread to inner surface of the sensitive layer, resulting in the fact that the gas molecules can only react with the particles near the sensitive layer, but not the particles inside, then the response is lower compared with that of calcination temperature at 350 °C.

In conclusion, the ZnO-350-M was successfully prepared by using methanol as reaction solvent with the calcination temperature at 350 °C and heating rate at 1 °C. Compared with other materials made in this experiment, the ZnO-350-M sensors show the optimal formaldehyde-sensing response compared with the others, which is 10 at 100 ppm, and it has fast response/recovery

time (4 s/4 s to 100 ppm) and good selectivity. These excellent performances can be attributes to the smaller size as well as hollow and porous structure of ZnO-350-M. Based on the reasons above, the ZnO-350-M gas sensor is a promising candidate for the formaldehyde sensor with good performance.

Declaration of competing interest

The authors declare that they have no known competing financial interests or personal relationships that could have appeared to influence the work reported in this paper.

Acknowledgments

The authors are grateful to National Natural Science Foundation of China (Nos. 61874048, 11874348, U1831113, 61974175, 61974055), Project of Science and Technology Plan of Jilin Province (No. 20180414020GH), Project of Jilin Provincial Development and Reform Commission (No. 2018C040-2) for the support to this work.

Appendix A. Supplementary data

Supplementary material related to this article can be found, in the online version, at doi:https://doi.org/10.1016/j.cclet.2019.12.014.

References

[1] Q. Zhang, H. Zhang, M.K. Xui, Z.R. Shen, Q. Wei, Chin. Chem. Lett. 24 (2014) 224–230.
[2] W. Zhou, Y.P. Wu, J. Zhao, et al., Inorg. Chem. 56 (2017) 14111–14117.
[3] S. Wicker, M. Guiltat, U. Weimar, A. Hémeryck, N. Barsan, J. Phys. Chem. C 121 (2017) 25064–25073.
[4] W. Sun, G. Sun, B. Qin, Q. Xin, Sens. Actuator. B -Chem. 128 (2007) 193–198.
[5] C.Y. Lee, C.M. Chiang, Y.H. Wang, R.H. Ma, Sens. Actuator. B -Chem. 122 (2007) 503–510.
[6] I.Y. Zhang, X. Huang, Q.Y. Shen, J.Y. Wang, G.H. Song, Chin. Chem. Lett. 29 (2018) 197–200.
[7] W. Li, X. Wu, N. Han, et al., Sens. Actuator. B -Chem. 225 (2016) 158–166.
[8] W. Xia, C. Mei, X. Zeng, et al., ACS Appl. Mater. Inter. 7 (2015) 11824–11832.
[9] N. Wei, H. Cui, X. Wang, et al., J. Colloid Interface Sci. 498 (2017) 263–270.
[10] Q.B. Zhu, X.Y. Shen, L.L. Wang, et al., Chin. Chem. Lett. 29 (2018) 1310–1312.
[11] S. Wang, P. Wang, C. Xiao, et al., Mater. Lett. 131 (2014) 358–360.
[12] A. Umar, S.H. Kim, Y.S. Lee, K.S. Nahm, Y.B. Hahn, J. Cryst. Growth 282 (2005) 131–136.
[13] R. Dang, X.L. Jia, P. Wang, et al., Chin. Chem. Lett. 28 (2017) 2263–2268.
[14] X. Lai, J.E. Halpert, D. Wang, et al., Energy Environ. Sci. 5 (2012) 5604–5618.
[15] Y. Li, X. Wang, C.Y. Xing, et al., Adv. Mater. 30 (2019) 1440–1444.
[16] B. Liu, H. Shioyama, H. Jiang, X. Zhang, Q. Xu, Carbon 48 (2010) 456–463.
[17] F. Zou, X. Hu, Z. Li, et al., Adv. Mater. 26 (2014) 6622–6628.
[18] G.W. Peterson, S.Y. Moon, G.W. Wagner, et al., Inorg. Chem. 54 (2015) 9684–9686.
[19] J.R. Li, Y. Ma, M.C. McCarthy, et al., Coord. Chem. Rev. 255 (2011) 1791–1823.
[20] P. Horcajada, C. Serre, M. Vallet-Regí, et al., Angew. Chem. 118 (2006) 6120–6124.
[21] G. Nickerl, I. Senkovska, S. Kaskel, Chem. Commun. 51 (2015) 2280–2282.
[22] B. Wang, A.P. Cote, H. Furukawa, M. O'Keeffe, O.M. Yaghi, Nature 453 (2008) 207–211.
[23] D.P. Volanti, A.A. Felix, M.O. Orlandi, et al., Adv. Funct. Mater. 23 (2013) 1759–1766.
[24] J. Tang, R.R. Salunkhe, J. Liu, et al., J. Am. Chem. Soc. 137 (2015) 1572–1580.
[25] R. Wu, D.P. Wang, J. Han, et al., Nanoscale 7 (2015) 965–974.
[26] F. Qu, C. Feng, C. Li, et al., Int. J. Appl. Ceram. Technol. 11 (2014) 619–625.
[27] L. Li, P. Gao, M. Baumgarten, et al., Adv. Mater. 25 (2013) 3419–3425.
[28] S.H. Yan, S.Y. Ma, W.Q. Li, et al., Sens. Actuator. B -Chem. 221 (2015) 88–95.
[29] W.C. Wang, F.Q. Liu, B. Wang, et al., Chin. Chem. Lett. 30 (2019) 1261–1265.
[30] H. Tian, H. Fan, M. Li, L. Ma, ACS Sens. 1 (2015) 243–250.
[31] C. Gu, Y. Cui, L. Wang, et al., Sens. Actuator. B -Chem. 241 (2017) 298–307.
[32] D. Wang, L. Tian, H. Li, et al., ACS Appl. Mater. Inter. 11 (2019) 12808–12818.
[33] W. Yang, P. Wan, X. Zhou, et al., Sens. Actuator. B- Chem. 201 (2014) 228–233.
[34] N. Zhang, S. Ruan, F. Qu, et al., Sens. Actuator. B -Chem. 298 (2019) 126887.
[35] X. Chu, T. Chen, W. Zhang, B. Zheng, H. Shui, Sens. Actuator. B -Chem. 142 (2009) 49–54.
[36] W.T. Koo, S.J. Choi, J.S. Jang, I.D. Kim, Sci. Rep. 7 (2017) 45074.
[37] A. Rothschild, Y. Komem, J. Appl. Phys. 95 (2004) 6374–6380.
[38] X. Gou, G. Wang, J. Park, H. Liu, J. Yang, Nanotechnology 19 (2008) 125606.
[39] P. Sun, C. Wang, J. Liu, et al., ACS Appl. Mater. Interfaces 7 (2015) 19119–19125.